Available online at www.sciencedirect.com
SCIENCE DIRECT
Polymer 46 (2005) 10405–10418
polymer
www.elsevier.com/locate/polymer

Rheological and mechanical comparative study of in situ polymerized and melt-blended nylon 6 nanocomposites

J. Tung[a], R.K. Gupta[b], G.P. Simon[a,*], G.H. Edward[a], S.N. Bhattacharya[b]

[a]*CRC for Polymers, School of Physics and Materials Engineering, Monash University, Vic. 3800, Australia*
[b]*Rheology and Materials Processing Centre, RMIT University, Melbourne, Vic. 3000, Australia*

Received 28 January 2005; accepted 13 August 2005
Available online 8 September 2005

Abstract

The rheological and mechanical properties of commercial neat nylon 6 and nylon 6 nanocomposites containing organically-modified montmorillonite (organoclays) produced by either in situ polymerization or melt-blending were investigated. The dynamic and steady shear, capillary and extensional viscosity of the neat nylon 6 and nylon 6 nanocomposite melts were studied, as well as the tensile properties of the solid material. X-ray diffraction (XRD) and transmission electron microscopy (TEM) indicated that the organoclays were largely very well exfoliated, although the lateral size scale of the platelets was different for each material. The in situ polymerized nanocomposite exhibited higher melt viscosity and higher tensile ductility than the melt-blended nanocomposite which was related to improved dispersion and polymer–silicate interactions for this material. Scanning electron microscopy confirmed that the nanocomposite failure surfaces showed more evidence of brittle behavior than the failure surfaces of neat nylon 6, and also that agglomerates of organoclay could be seen easily in the fracture surface of the melt-blended nanocomposite, but not to the same degree as in the in situ polymerized nanocomposite. This is in addition to very fine, individually-dispersed silicate laminates that form in each case.

Keywords: Nylon 6; Nanocomposites; Dispersion techniques

1. Introduction

Polymer layered-silicate nanocomposites represent a potentially very advantageous alternative to conventional polymer composites due to the large surface area and high aspect ratio of the incorporated layered silicates. As a result, it is possible to achieve a high degree of stiffness increase and moderate strengthening with very low loading of organoclays, thus reducing the weight of the composite material. The property enhancement is largely due to the ability of layered silicates to exfoliate, and the for an intimate dispersion of the nanometer-thick silicate layers to occur within the polymer matrix.

The incorporation of organoclays in polymer matrices has been the subject of much recent research. Interest has focused on understanding and developing polymer nanocomposites for a wide range of applications using a variety of polymers, such as epoxy resins [1], EVA [2], polypropylene [3] and so on. Nylon 6 is one of the few common polymers that readily forms well-exfoliated nanocomposites. Nylon 6 layered silicate nanocomposites can be prepared using either in situ polymerization [4–6], melt intercalation [6–8] or solution mixing [9,10]. Generally, in situ polymerization and melt intercalation are the two main preparative strategies, where in situ polymerization involves dispersion of layered silicates into monomer followed by polymerization, whilst melt intercalation involves mechanical blending of clay in the molten polymer, and relies on reptation of polymer molecules into the galleries of the layered silicates and the shearing motion. The melt intercalation technique is usually achieved using an extruder or internal mixer, the efficiency of delamination of the galleries of layered silicates depending on the nature of the mixing motion. This technique has been reported to be more economical and straightforward than the in situ polymerization technique, but full exfoliation of silicate layers is not always achievable [11–13].

* Corresponding author. Tel.: +61 3 99054936; fax: +61 3 99054940.
E-mail address: george.simon@eng.monash.edu.au (G.P. Simon).

0032-3861/$ - see front matter © 2005 Elsevier Ltd. All rights reserved.
doi:10.1016/j.polymer.2005.08.043

Whilst extensive work concerning melt compounding to achieve a high level of exfoliation has been reported, relatively little work has been reported on in situ polymerized materials, particularly concerning the rheology–morphology–property relationships. According to Incarnato et al. [14], viscoelastic measurements in the melt (rheometry) is a highly sensitive way to probe the nanoscale structure of the hybrids. It was reported that the layered silicate nanocomposites exhibit a transition from liquid-like to solid-like behavior in the linear viscoelastic region, with relatively small changes to the intercalated and exfoliated structure [15–17,2]. Moreover, Krishnamoorti et al. [18] showed that a layered silicate nanocomposite exhibits shear thinning behavior in the dynamic frequency sweep measurement at significantly smaller strain amplitudes than the neat polymer. Therefore, detailed rheological studies are important to allow evaluation of the dispersion techniques of polymer nanocomposites.

In this paper, the rheological and mechanical properties of two commercially-available nylon 6 nanocomposites are investigated, one of which was produced by in situ polymerization and the other by melt-blending. In addition to shear rheometry, extensional viscosity results are given, the first time such data has been presented for nylon 6 nanocomposites. The exfoliation level of the nanocomposites is evaluated using a common approach, i.e. wide angle X-ray diffraction (WAXD) and transmission electron microscopy (TEM). It is interesting to compare the rheological measurements, with the more widely-used XRD and TEM techniques, and relate these to mechanical performance. The thermal, morphological and mechanical properties of the neat polymer and the different nanocomposites are examined using differential scanning calorimetry (DSC), scanning electron microscopy (SEM) and by tensile measurements.

2. Experimental

2.1. Materials

The details of the neat nylon 6 and the nylon 6 organoclay nanocomposites used in this study are summarized in Table 1. The neat nylon 6 was obtained from the RTP Company, whilst the in situ polymerized nylon 6 nanocomposite was obtained from Honeywell, and the composite made through melt intercalation from the RTP Company. In this paper, they are labelled as Nylon 6, Nylon 6 IS and Nylon 6 MB, respectively.

Table 1
Details of materials used in this study

Material	Commercial grade	M_n	Supplier
Nylon 6	RTP 0200 A	18,000	RTP Company
Nylon 6 IS	Capron 2908	17,131	Honeywell
Nylon 6 MB	RTP 0299 A	18,000	RTP Company

Since the materials are obtained commercially, the nature of the clay surface treatment and the actual loading of organoclays in the polymer are unknown. It is of interest to know the organoclay concentration prior to investigating and comparing the nanocomposites. The precise weight of organoclays in the nylon 6 nanocomposites was measured using a Setaram TG92 thermogravimetric analysis (TGA), operating at a heating rate of 30 K/min in an argon gas atmosphere. The sample was heated from 50 to 1000 °C, and the remaining weight of mineral montmorillonite (MMT) ash was measured.

2.2. Wide angle X-ray diffraction (WAXD)

Wide angle X-ray diffraction (WAXD) measurements were performed from compression molded plaques. These experiments were measured using a Philips X-ray generator with Cu ($\lambda = 1.542$ Å) radiation, at 30 kV accelerating voltage, 30 mA current, and were recorded in transmission mode at room temperature.

2.3. Thermal properties

Thermal transitions of nylon 6 and its nanocomposites were determined using a Pyris 1 differential scanning calorimetry (DSC), operating at a scan rate of 10 °C/min in a nitrogen atmosphere. The granular samples were first heated from 25 to 300 °C and held at this temperature for 3 min to remove their thermal history. The samples were then cooled to 25 °C and held for 2 min before re-heating to 300 °C. The values of crystallization temperature (T_c), melting temperature (T_m) and melting enthalpy ΔH_m were determined from the cooling and second heating scans.

2.4. Rheological

Rheological measurements were performed using a rotational rheometer (Rheometrics, Inc.) with parallel plate geometry (plate diameter = 25 mm). The compression-molded plaques were used for measurements at 225 and 235 °C after drying at 80 °C in a vacuum oven for 24 h, in order to prevent moisture-induced degradation phenomena. All measurements were performed with a force transducer with a range of 0.2–200 g-cm torques. Typical samples thickness ranged from 1.2 to 1.5 mm. The rheological measurements were carried out, as follows:

i. Steady shear rate tests over a shear rate ranges from 0.05 to 1.75 s^{-1}
ii. Dynamic strain sweep tests to confirm the linearity of viscoelastic region and
iii. Dynamic frequency sweep test over a frequency range of 0.1–100 rad/s.

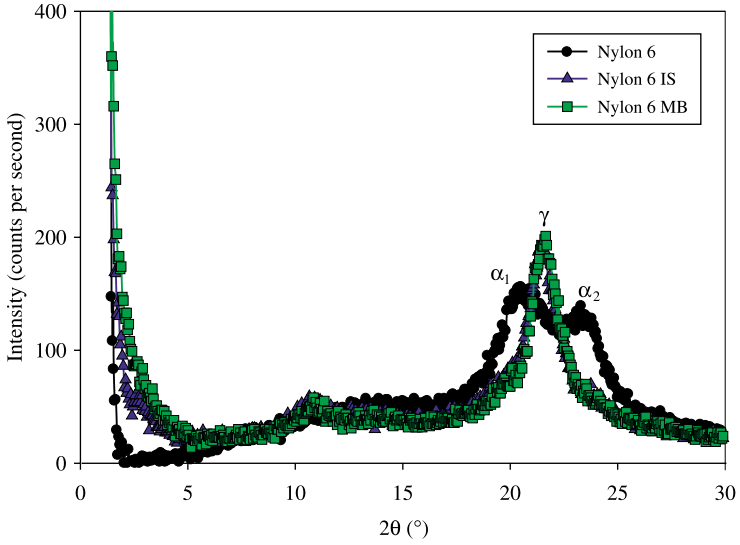

Fig. 1. XRD profiles of neat nylon 6 and nylon 6 nanocomposites.

Shear viscosity measurements at higher shear rates were measured using a Rosand twin barrel capillary rheometer RH7-2 (diameter = 1 mm, die length = 20 mm). The tests were conducted at a temperature of 235 °C.

The extensional viscosity behavior of the materials was measured at 225 and 235 °C with a rheometric extensional rheometer (RME). The rectangular samples (height = 1.2 mm, width = 7.0 mm, length = 60 mm) were cut from compression-molded plaques. RME is a commercial extensional rheometer, details of which are given elsewhere [19].

2.5. Injection molding

Dumbbell shape tensile specimen (ASTM D638) of the materials were injection molded with a Battenfeld™ model Plus 350-75 35ton injection molding machine (screw diameter = 30 mm, L/D ratio = 13.5:1, maximum injection pressure = 109.4 MPa) along with a Yann Bang model YBM-I-P mold temperature controller. The barrel temperature was set at 268 °C, mold temperature of 80 °C, injection pressure of 25 MPa, holding pressure of 22 MPa, cooling time of 30 s, screw rotational speed of 55 rpm and back pressure of 9 MPa.

2.6. Mechanical testing

Tensile specimens were conditioned at 25 °C for at least a week following processing before mechanical property measurements were performed. The values reported reflect an average from five measurements. Tensile testing was done using an Instron 4505 with a 5 kN load cell at a crosshead speed of 50 mm/min.

Table 2
Summary of remaining mineral MMT ash in in situ and melt-blended nanocomposites

Material	Remaining mineral MMT ash (wt%)
Nylon 6 IS	2.9 ± 0.2
Nylon 6 MB	3.5 ± 0.5

2.7. Scanning electron microscopy

Fracture surfaces of tensile failure specimens were imaged using a FEI™ Quanta 200 environmental scanning electron microscopy (SEM), at 20 kV, low vacuum and back scattering light condition. The organoclays on the fracture tensile surface were detected using an energy dispersive X-ray (EDX) elemental analysis tool.

2.8. Transmission electron microscopy (TEM)

The morphology of nylon 6 nanocomposites was imaged using a Jeol™ model 1010 transmission electron microscope (TEM) at 100 kV accelerating voltage. Ultra-thin sections (60 nm in thickness) were cut from compression molded plaques under cryogenic condition using a Leica–Reichert Ultracut microtome. The sample and knife temperatures were cryogenically cut with a diamond knife Diatome Cryo-diamond knife (35° edge) at a temperature of −155 and −160 °C, respectively.

3. Results and discussion

3.1. Materials

Table 2 shows the results of thermogravimetric analysis (TGA) measurements in terms of the quantity of remaining weight percentage of mineral montmorillonite (MMT) ash from either the in situ polymerized or melt-blended nylon 6 nanocomposites. Table 2 shows that the remaining weights

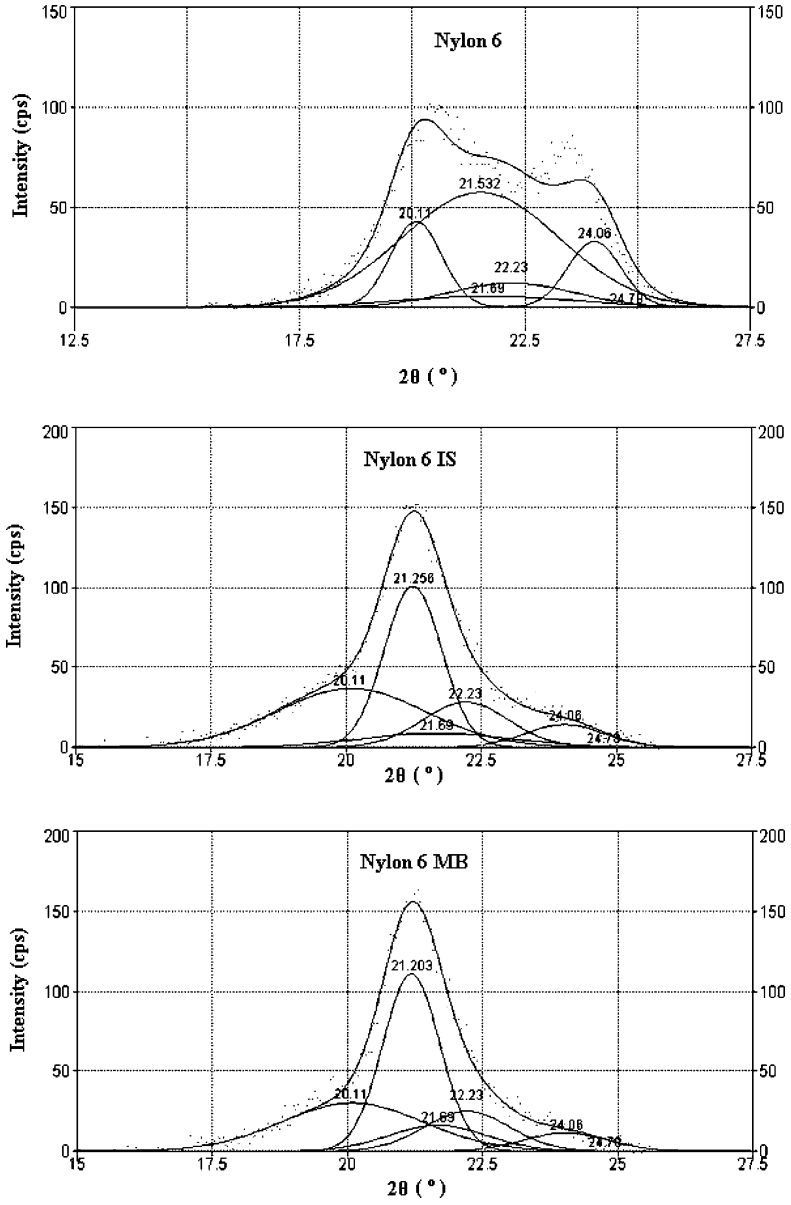

Fig. 2. WAXD intensity—2θ(15–25°) patterns were fitted using the profile fitting program PeakFit™ with a Gaussian–Lorentzian peak shape and are fitted with an R^2 determination of above 0.97. The profile fitting technique is used deconvolute the amorphous and crystalline phases. The 2θ positions of α and γ crystalline phases are located at 20.11° (α200), 21.69° (γ001), 22.23° (γ200), 24.06° (α002) and 24.78° (α202) with a wavelength of 1.542 Å.

of mineral MMT ash for the in situ and melt-blended nanocomposites are ca. 2.9 wt% ± 0.2 and 3.5 wt% ± 0.5, respectively. These values are an average of 10 measurements each. The clay concentrations of both nanocomposites are clearly quite similar. Being commercial materials, the precise type and amount of organoclay surface treatment are unknown, but generally in nanocomposites organic modification comprises some 20–30 wt% of weight of the organically-modified clay (or some 70–80 wt% clay). This makes it likely that there is between 4 and 5 wt% of treated organoclay in both types of nanocomposite.

Table 3
Crystallinity data obtained from the WAXD patterns ($2\theta = 15$–25°)

Material	% α	% γ	% amorphous	Relative proportional ratio of γ in total crystalline phases
Nylon 6	30	21	49	0.41
Nylon 6 IS	13	27	60	0.68
Nylon 6 MB	10	28	62	0.74

3.1.1. X-ray diffraction

Fig. 1 shows X-ray diffraction (XRD) profiles of samples taken from compression molded plaques and are analyzed using the profile fitting program PeakFit™ (AISN Software Inc.) and the crystalline and amorphous reflections results are displayed in Fig. 2. Table 3 summarizes crystallinity data from such reflection profiles. The XRD profiles

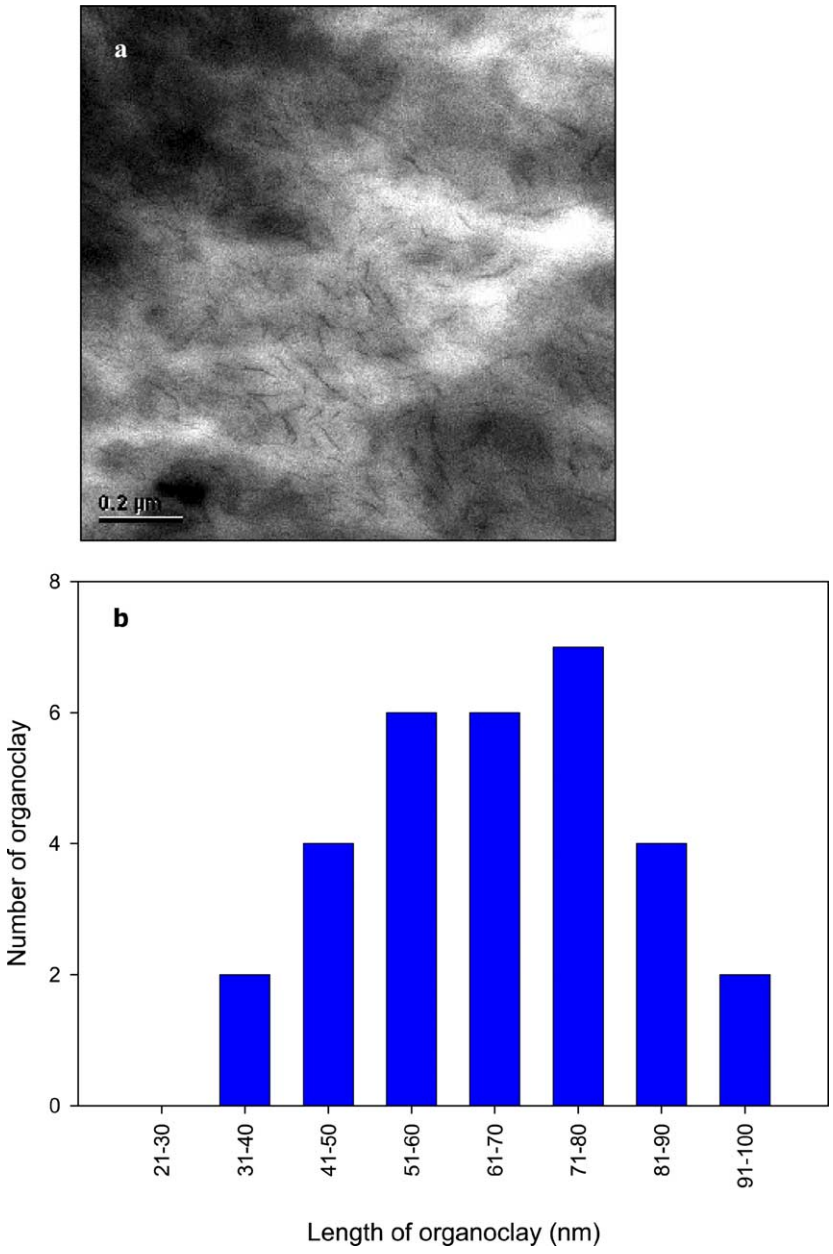

Fig. 3. (a) TEM micrograph of in situ polymerized nanocomposites, and (b) organoclay platelet length distribution measurement obtained from the above TEM micrograph.

presented in Fig. 1 permit the examination of crystallinity behavior and effect of organoclay exfoliation level. All samples contain peaks at $2\theta \approx 20.11$, 24.06 and 24.78°, corresponding to the α crystalline phases, $2\theta \approx 21.69$ and 22.23° indicative of the γ crystalline phases and $2\theta \approx 21.4 \pm 0.5°$ representing the broad amorphous peak. Similar behaviour in the nylon 6 nanocomposites has been observed by Varlot et al. [20], Devaux et al. [21] and Fornes et al. [22]. The addition of organoclay results in significant enhancement of the γ-form crystal structure, and alters the relative proportions of the α- and γ-form crystallinity of the polymer. The nanocomposites consist of a much higher content of γ, in the range of 27–28% compared to neat nylon 6 with 21%. VanderHart et al. [23,24] studied the γ-form crystal structure using DSC and solid state NMR, and concluded that the γ-crystallites were found residing near the polyamide/clay interface, and have been shown to have a lower melting point than the α-crystals [22]. The in situ polymerised nanocomposite demonstrates a lower proportion of γ crystalline phase, which results in a higher average melting temperature than the melt-blended nanocomposite (Section 3.1.3).

Neither of the nanocomposites show any Bragg peak at below $2\theta \approx 5°$, which indicates that there is a good

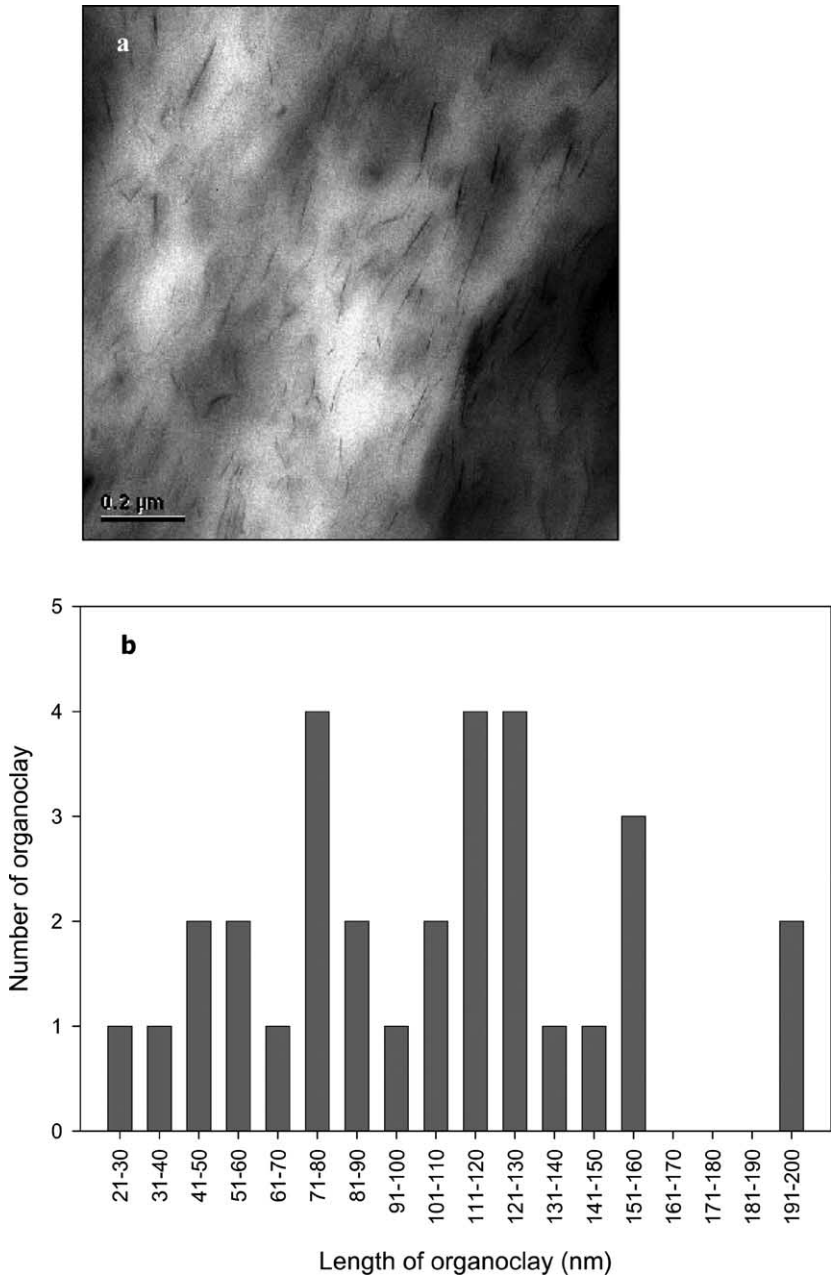

Fig. 4. (a) TEM micrograph of melt-blended nanocomposites, and (b) organoclay platelet length distribution measurement obtained from the above TEM micrograph.

exfoliation level of silicate layers in the polymer matrix. The polymer chains penetrate into the galleries of layered silicates, delaminate and disperse the individual silicate layers in the polymer matrix, either during the polymerization process or through melt-blending.

Table 4
Organoclay platelet length distribution measurements of both the nanocomposites

Material	Average length (nm)	Length distribution range (nm)
Nylon 6 IS	65	31–100
Nylon 6 MB	100	21–200

3.1.2. Transmission electron microscopy

Figs. 3 and 4 show TEM micrographs and organoclay platelet length distribution measurements of in situ polymerized and melt-blended nylon 6 nanocomposites.

A summary of the organoclay length distribution measurements is shown in Table 4. The average length of the clay platelets appears to be approximately 65 nm. Fig. 4 shows the clay platelets largely disperse individually in the melt-blended nanocomposite, and the average length of organoclay is at ca. 100 nm. The clay platelets in the in situ polymerized sample are slightly shorter and a little better dispersed as compared to those of the melt-blended

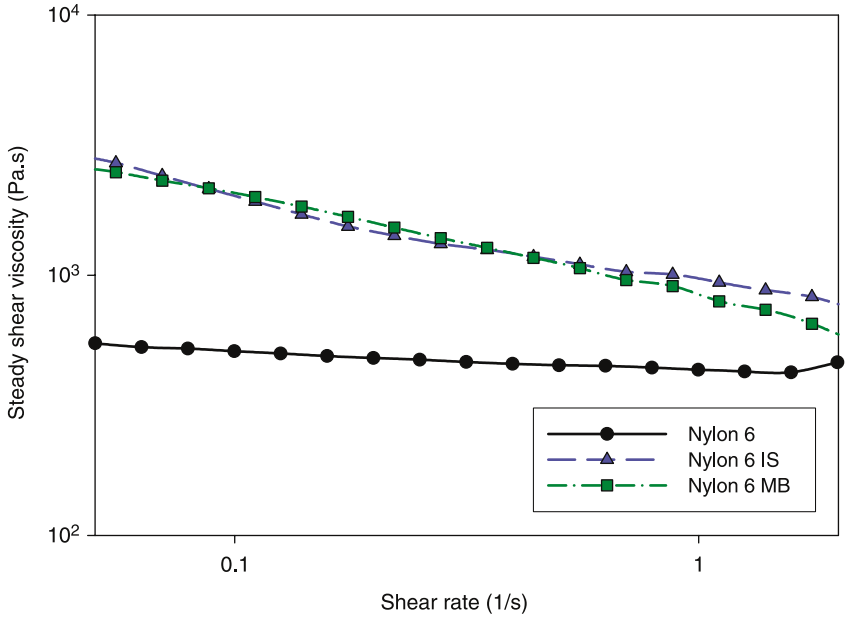

Fig. 5. Steady shear viscosity at 225 °C.

nanocomposite. These differences in length may be due to differences in the initial clays used, but the degree of dispersion likely reflects the ease with which monomer can ingress the galleries and cause expansion due to polymerization, as opposed to polymer melt diffusion.

3.1.3. Thermal properties

Table 5 shows melting and crystallization temperatures of differential scanning calorimetry (DSC) for nylon 6 and nanocomposites. The DSC measurements indicate that the in situ polymerized nanocomposite has a slightly higher melting temperature than the melt-blended nanocomposite. The difference in melting temperature may simply reflect the changes in crystallite thickness and its distribution in the polymer matrix [22,25]. From the previous XRD section, the peak fitting profiles show that the in situ polymerized nanocomposite consists of a lower relative proportion of γ crystalline phase than the melt-blended nanocomposite, and the γ-crystal is reported to have a lower melting point than the α-crystal form [22], and thus the relatively smaller proportion of γ crystalline phase increases the apparent melting point of the in situ nanocomposite.

Table 5
Differential scanning calorimetry data of samples under non-isothermal heating and cooling conditions (10 °C/min)

Material	Second heating			Cooling peak
	T_m (°C)	ΔH_m (J/g)	Degree of crystallinity (%)[a]	T_c (°C)
Nylon 6	221.4	54.7	22.8	174.3
Nylon 6 IS	224.8	46.5	19.4	179.5
Nylon 6 MB	222.3	48.7	20.3	183.0

[a] Degree of crystallinity is calculated by the ratio of $H_m/\Delta H_m^o$ where ΔH_m^o is 240 J/g [22].

As seen in Table 5, the addition of organoclays results in an increased of crystallization temperature. The crystallization temperatures of neat nylon 6, in situ polymerized and melt-blended nanocomposites are 174.3, 179.5 and 183.0 °C, respectively. Clearly, the incorporation of organoclays increases the crystallization temperature, the small clay size allowing it to act as nucleating agent, reducing the degree of undercooling and thus final crystal size.

On the other hand, the nanocomposites demonstrate a slightly lower degree of crystallinity compared to the neat nylon 6. The degree of crystallinity of neat nylon 6, in situ polymerized and melt-blended nanocomposites was 22.8, 19.4 and 20.3%, respectively. One possible explanation of the lower crystallinity in the nanocomposites is the inability of polymer chains to be fully incorporated into growing crystalline lamella. The presence of silicates layers restricts large crystalline domains from forming due to limited space and restrictions imposed on polymer chains by a large number of disordered silicate platelets, this leads to smaller crystallite structures and more defect-ridden crystalline lamella.

3.2. Rheological studies

3.2.1. Steady shear rheology

For polymer composite systems, the size, shape and concentration of the filler can have a significant effect on the rheological properties in the melt state. Generally, the viscosity of molten reinforced composites exhibit shear thinning behavior at high shear rates. Surprisingly, there have been relatively few detailed studies of the rheological

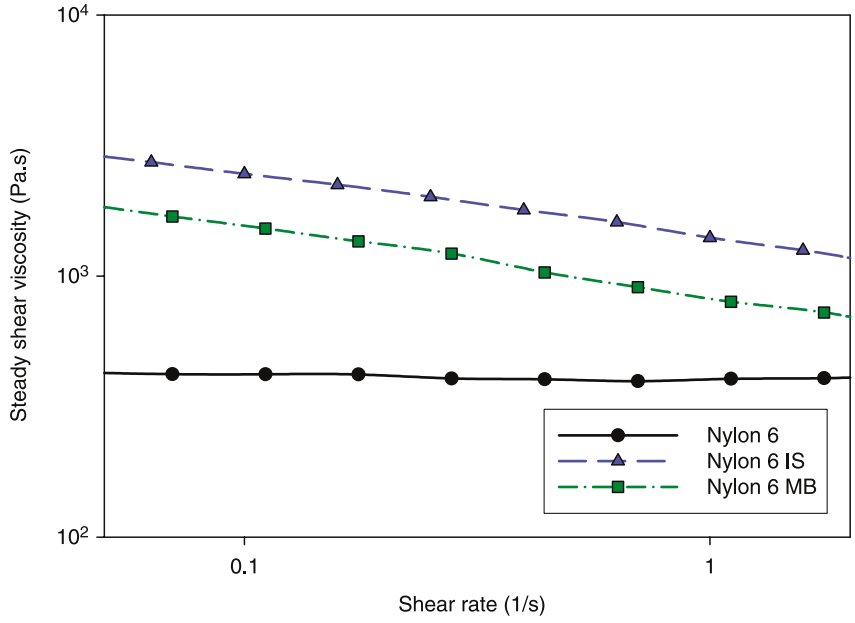

Fig. 6. Steady shear viscosity at 235 °C.

properties of nylon 6 nanocomposites formed from organoclays.

Figs. 5 and 6 show the steady shear viscosity behavior of neat nylon 6 and the nanocomposites at temperature of 225 and 235 °C. The rheological behavior at 235 °C shows more distinct difference between the in situ and melt-blended nanocomposites. The nanocomposites formed from the organoclays exhibit shear thinning behavior, whilst the neat nylon 6 exhibits Newtonian behavior. It is of interest to note that the absolute value of the melt viscosity of the organoclay nanocomposites is significantly higher than that of neat nylon 6, particularly at the low shear rate. The high, zero shear rate viscosity of nylon 6 nanocomposites indicates that at low shear rates, the nanostructure of these materials consists of percolated network superstructure of the exfoliated layers in terms of the effect of the clay on polymer properties. The significant lowering of the critical concentration for percolation behavior is due to the anisotropy of the tactoids and the small size of the individual layers that prevent free-rotation of these elements. It is noteworthy that the in situ polymerized nanocomposite exhibits higher shear viscosity throughout the entire range of shear rate investigation, particularly at the temperature of 235 °C. This higher shear viscosity

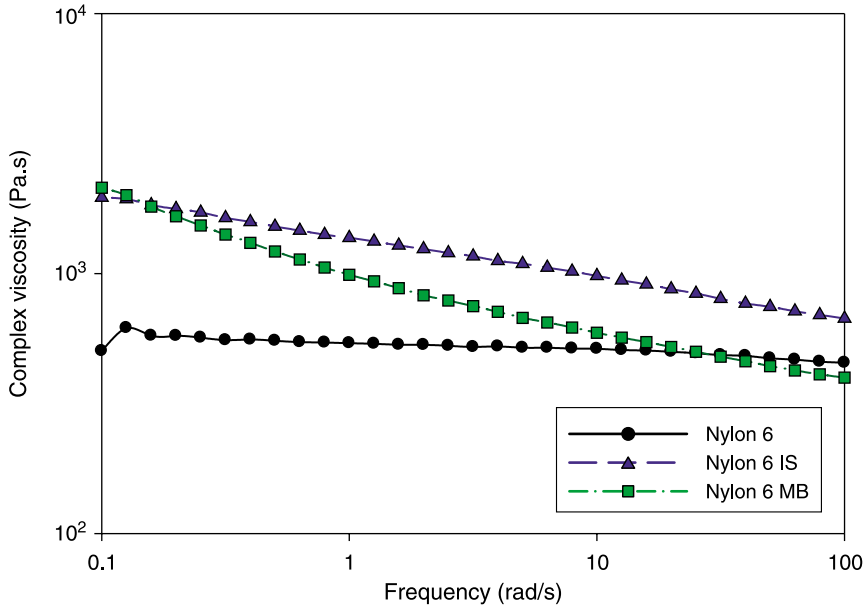

Fig. 7. Complex viscosity from oscillatory rheometry at 225 °C.

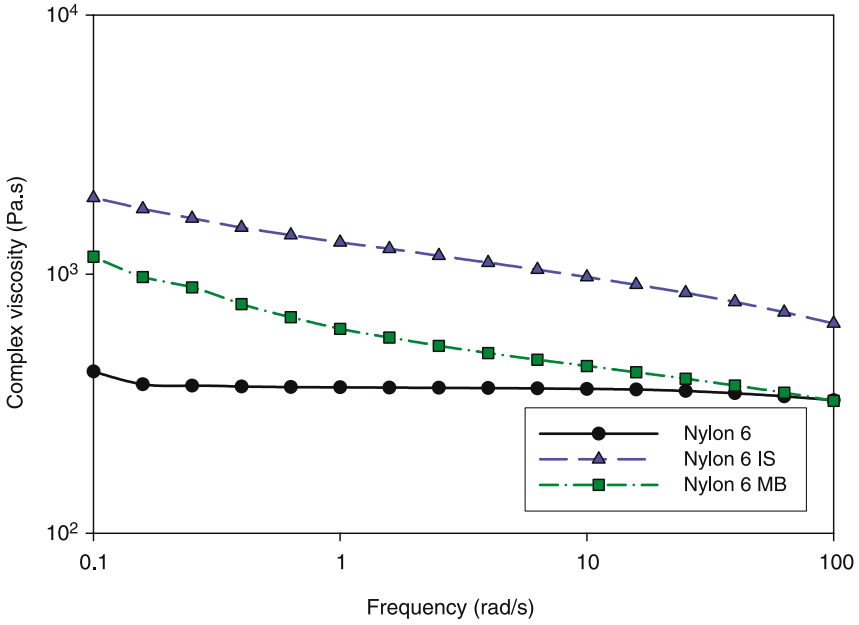

Fig. 8. Complex viscosity from oscillatory rheometry at 235 °C.

exhibited by the in situ nanocomposite likely results from the greater clay dispersion and exfoliation levels for in situ polymerization method, coupled with stronger polymer–silicate interactions due to the in situ polymerization technique where the usual clay treatment, including organo-ion based on dodecanoic acid means that the ε-caprolactam actually chemically bonds to the organo-ion (as opposed to physical interactions in organo-ions used on silicates for melt blending). In addition, the small size of the clays—in terms of both width and length—leads to high surface areas and thus only a few wt% of material causes the viscosity increase. However, the distance between clay layers that is also a key aspect. As seen from Figs. 3(a) and 4(a), this is some 50–100 nm between clay layers, and this is, of the order of the entanglement density of the nylon 6 melt.

3.2.2. Dynamic rheological properties

Figs. 7 and 8 show that both nanocomposites exhibit higher complex viscosity than neat nylon 6 at low frequencies, at temperatures of 225 and 235 °C, respectively. The neat nylon 6 exhibits Newtonian behavior, while the nanocomposites exhibit decreasing complex viscosity with increasing frequency. As mentioned above, as well as

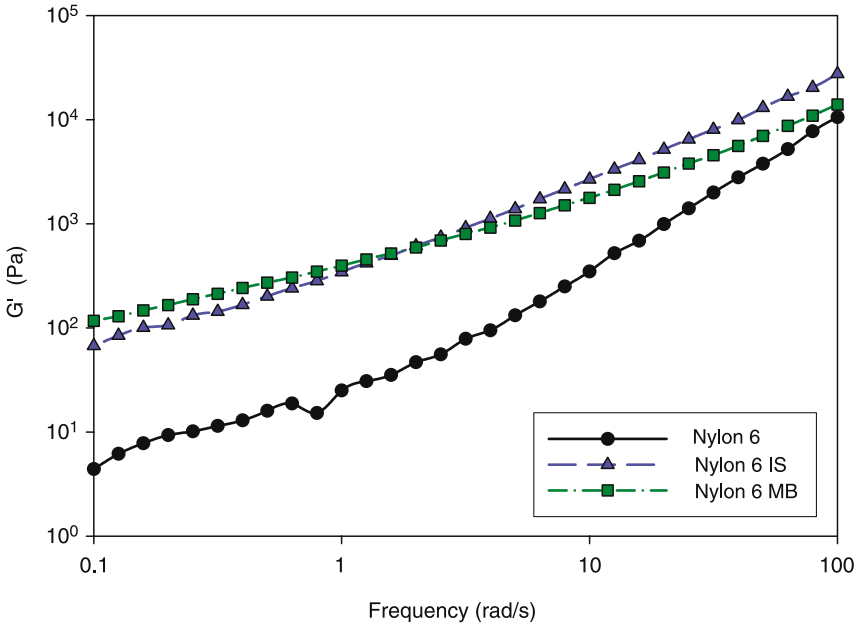

Fig. 9. Storage modulus from oscillatory rheometry at 225 °C.

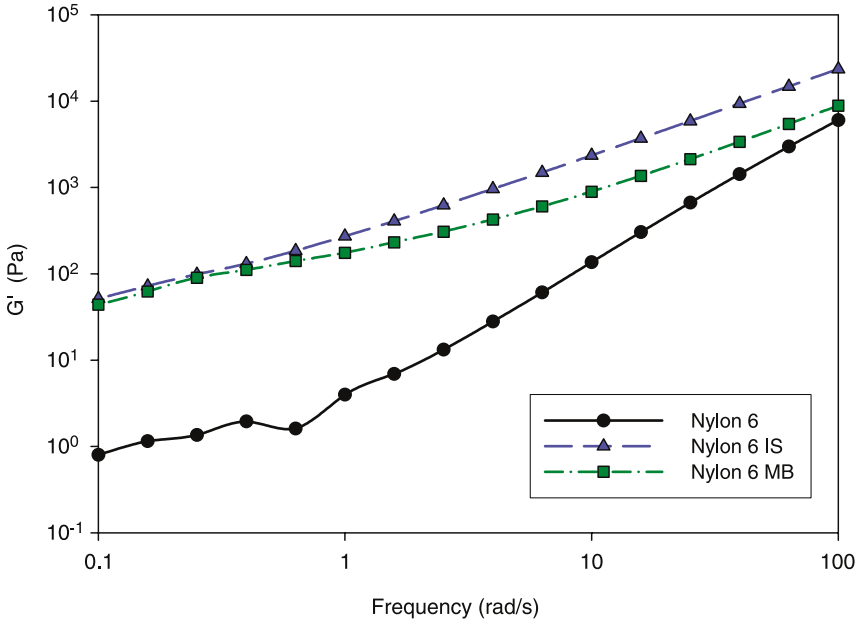

Fig. 10. Storage modulus from oscillatory rheometry at 235 °C.

the organoclay particles being nano in size-scale, they are separated from each other by the order of a few nylon entanglement lengths of some 100 nm (Figs. 3 and 4). Thus the clay can contribute to, and possibly impede entanglement mobility, and when sheared the deformation of the clay can modify the entanglement network and result in shear thinning.

Figs. 9 and 10 show a viscoelastic dynamic oscillatory response as measured by the storage modulus (G′) at temperatures of 225 and 235 °C, respectively. Figs. 11 and 12 show the viscoelastic response as measured by the loss modulus (G″) at temperatures of 225 and 235 °C, respectively and solid-like behavior can be seen from the dynamic oscillatory response. Both nanocomposites demonstrate higher storage moduli at both low and high frequencies and exhibit more solid-like behavior than the neat nylon 6, and similar trends are observed in the Figs. 11 and 12. It is noteworthy that the melt-blended nanocomposite appears to have more solid-like behavior than the in situ nanocomposite. One possible explanation for this difference is the different organoclay length distributions. The silicate layers of the melt-blended nanocomposite are found to be longer than in the in situ nanocomposite, judging from the TEM photomicrograph in Fig. 4. This increases the

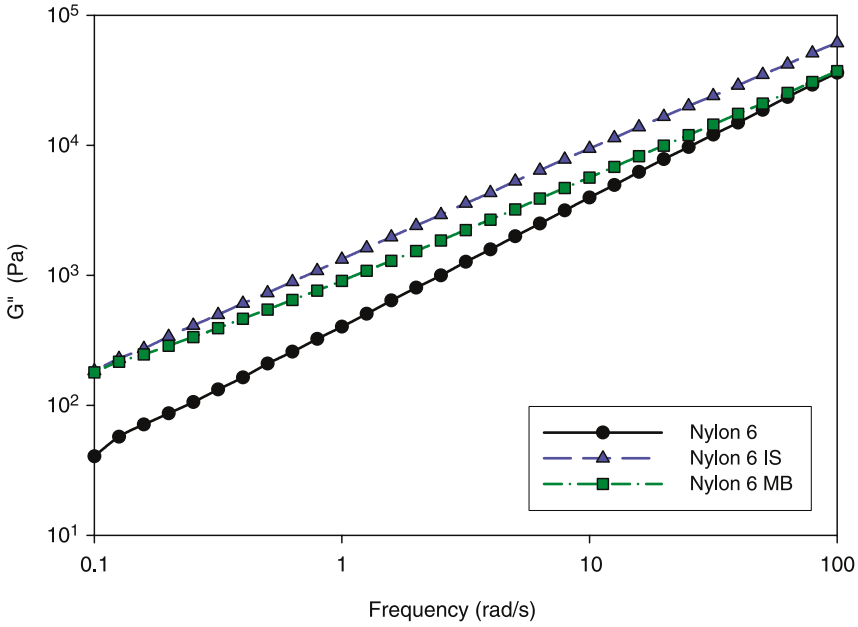

Fig. 11. Loss modulus from oscillatory rheometry at 225 °C.

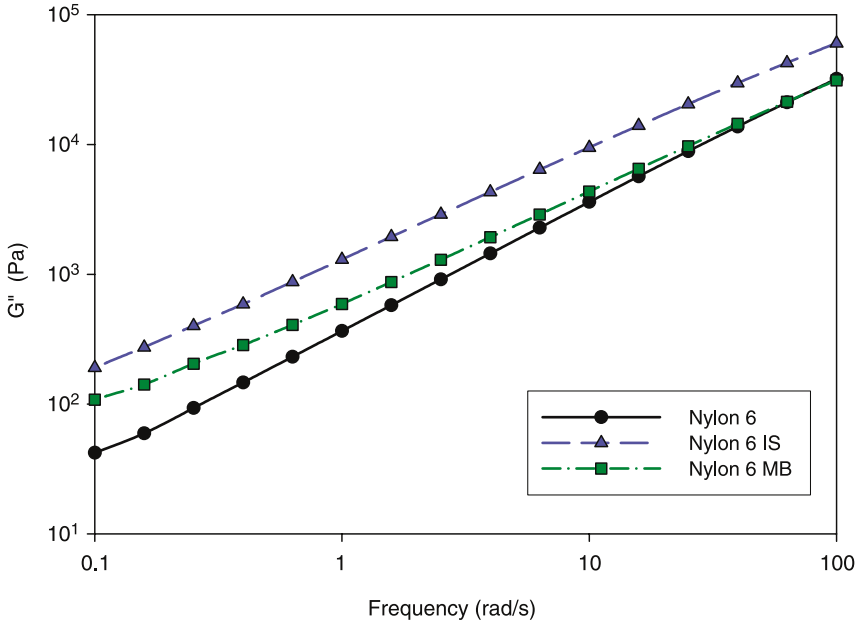

Fig. 12. Loss modulus from oscillatory rheometry at 235 °C.

probability of clay–clay interaction in the melt-blended nanocomposite during oscillatory motion and hence, increases the solid-like behavior of the melt-blended nanocomposite.

3.2.3. Capillary rheology

Fig. 13 shows the shear viscosity behavior for neat nylon 6 and the nanocomposites obtained from capillary rheometry. The in situ nanocomposite demonstrates a higher shear viscosity than the melt-blended nanocomposite, similar to the observations from the steady shear viscosity measurements. The high shear viscosity implies strong interfacial bonding of silicate layers with the matrix. In the case of the melt-blended nanocomposite, a lower shear viscosity occurs due to the organoclays being physically attached to the polymer matrix, compared to the stronger chemically attached between clay and polymer in the in situ nanocomposite.

3.2.4. Extensional viscosity rheology

Fig. 14 shows the extensional viscosity measurements as a function of strain for both nanocomposites at 225 °C.

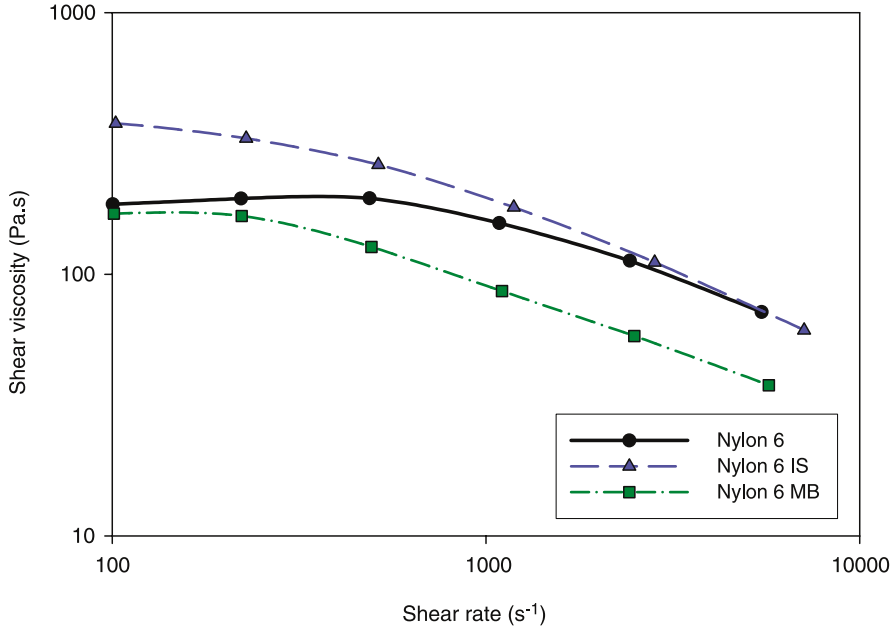

Fig. 13. Capillary shear data at 235 °C.

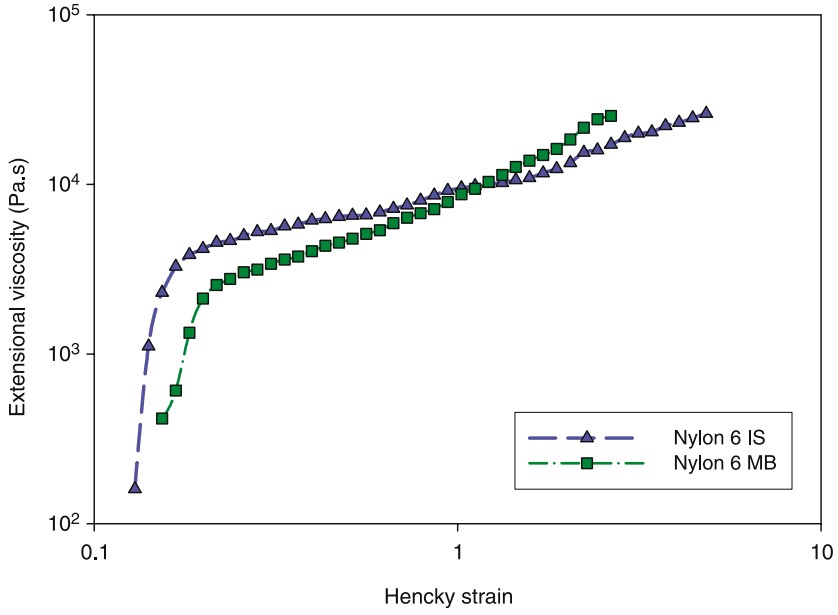

Fig. 14. Extensional viscosity for both nanocomposites with strain rate 1.0 s^{-1} at 225 °C.

Attempts to measure the extensional viscosity at 235 °C failed because it was very difficult to pull the specimens apart before they started to flow in the grips immediately after placing the rectangular specimens inside the heating chamber. This is because this temperature is a long way above the glass transition temperature of about 47 °C, and thus a very low viscosity melt is obtained.

The extensional viscosity results in Fig. 14 indicate that the nanocomposites exhibit mild strain hardening behavior. Both the nanocomposites show strain hardening up to about 0.2 Hencky strain, and little strain hardening above 0.2 Hencky strain. Beyond this strain value, the silicate layers are oriented in the uniaxial flow field direction, and the nanostructure of silicate layers makes no further contribution to the strain hardening behavior.

The in situ polymerized nanocomposite has a higher extensional viscosity than the melt-blended nanocomposite, particularly at low strains. High extensional viscosity implies a stronger network formation between the silicate layers and polymer matrix, leading to a resistance to flow during stretching of polymer chains. The in situ polymerized nanocomposite exhibits a higher extensional viscosity since the silicate layers are chemically attached to the polymer matrix. The melt-blended nanocomposite

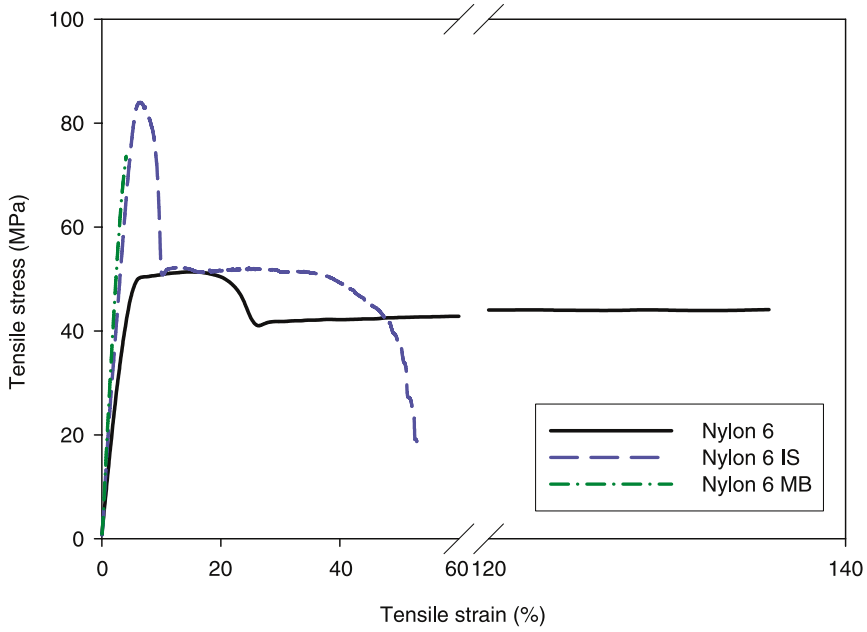

Fig. 15. Stress–strain curves for neat nylon 6 and nylon 6 nanocomposites.

demonstrates less resistance to flow because the silicates layers are only physically attached to the polymer matrix. Furthermore, the silicate layers of in situ polymerization process are dispersed a little more effectively than for the melt-blending technique.

3.3. Mechanical properties

Typical stress–strain diagrams for nylon 6 and nanocomposites are shown in Fig. 15 and a summary of the mechanical properties of these materials is shown in Table 6. As can be seen from the data, the tensile modulus and ultimate strength of the nanocomposites are substantially increased relative to the neat nylon 6, but with a reduced strain-to-failure. The organoclays thus enhance the ultimate tensile strength, whilst reducing the ductility. The melt-blended nanocomposites exhibit a lower tensile strength than the in situ polymerized nanocomposite. The neat nylon 6 elongates to a very large strain-to-failure, but the melt-blended nylon 6 shows very brittle behavior. The in situ nanocomposite shows a greater degree of ductility than that the melt-blended nanocomposite. It can be seen that the dispersion and adhesion between the clay and matrix are important factors influencing the mechanical behavior.

Fig. 16 shows an ESEM micrograph of the fracture surface of neat nylon 6 which exhibits ductile plastic deformation. The in situ polymerized nanocomposite fracture surface (Fig. 17) exhibits some degree of ductile plastic deformation, whilst the melt-blended nanocomposite fracture surface (Fig. 18) demonstrates a more brittle fracture. The dispersion of organoclay agglomeration is observed easily in the fracture surface of the melt-blended nanocomposite. Indeed, very little evidence of organoclay agglomerates can be detected by the EDX on the fracture surface of in situ nanocomposite. Although the incorporation of organoclays into polymer matrix by melt-blending process is a promising approach for forming nanocomposites, it remains less effective in obtaining total organoclay dispersion. The melt-blending technique relies on the shear-induced delamination of the organoclays for dispersion, which become swollen and intercalated in the presence of the polymer melt. The agglomerates occur when the cohesive forces of the agglomerates are exceeded by the hydrodynamic separating forces applied by the matrix fluid [12]. This is then followed by peeling of these layers and the aggregates may lead to the inferior properties [26]. Indeed, any remaining agglomerates of organoclay act as stress concentrators, initiating the failure when load is applied to the tensile specimen.

Table 6
Results of tensile properties of neat nylon 6 and nylon 6 nancomposites

Material	Tensile modulus (GPa)	Ultimate tensile strength (MPa)	Strain-to-failure (%)
Nylon 6	3.6±0.3	51.4±5.0	135.7±10.2
Nylon 6 IS	15.1±1.1	84.1±8.2	53.2±12.5
Nylon 6 MB	18.0±1.5	73.6±5.1	4.1±0.3

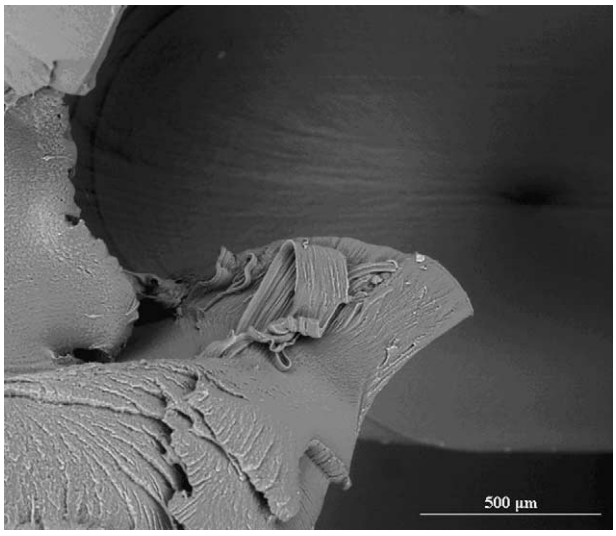

Fig. 16. Tensile fractured surface of neat nylon 6.

4. Conclusions

The method of clay dispersion is an important factor affecting the rheological, thermal and mechanical properties of nylon 6 nanocomposites. A broad organoclay length distribution is observed in composites prepared by the melt-blending technique because of extensive damage to the silicate layers likely due to the high shearing forces generated by the screw rotating at the top of the screw flight. The thermal transitions of melt-blended nanocomposites demonstrate a lower melt temperature than the in situ nanocomposite because of the higher relative proportion of γ-form crystals and imperfect crystallites formed in the melt-blended nanocomposite. In rheological measurements, the melt-blended nanocomposite exhibits more shear thinning than the in situ nanocomposite, mainly because

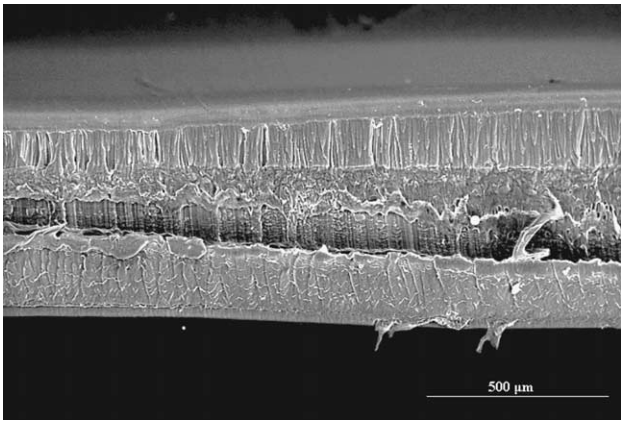

Fig. 17. Tensile fractured surface of in situ polymerized nanocomposites.

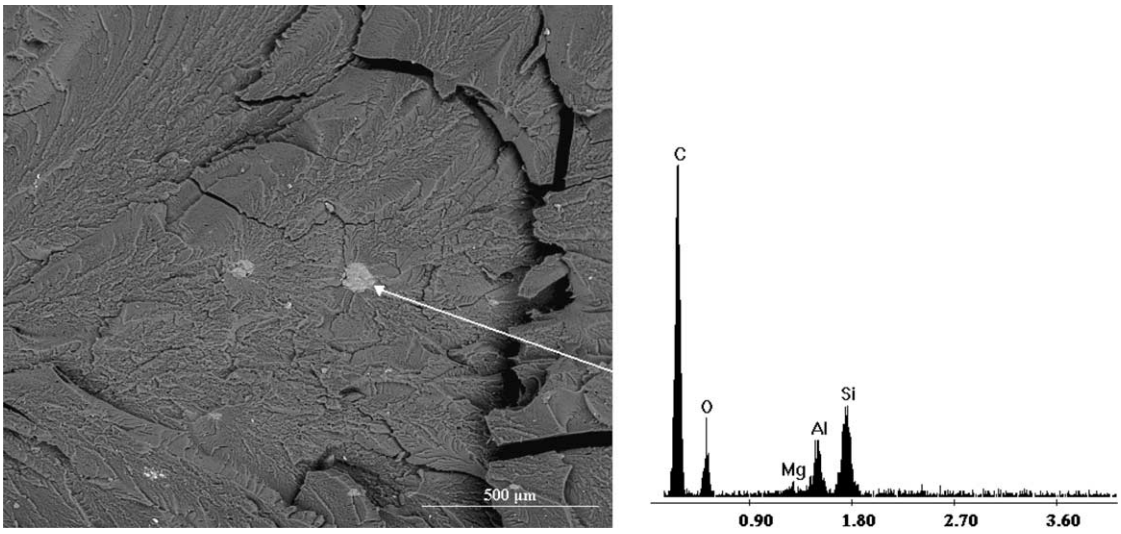

Fig. 18. ESEM micrograph and EDX of melt-blended nanocomposites.

the bonding force between the clay platelets and polymer matrix is primarily physical interactions for the melt-blended nanocomposites as compared to chemical bonding for the in situ composites. This likely also causes better dispersion for the in situ materials. The dispersion technique also demonstrates a significant effect on the mechanical properties. Better dispersion (achieved by the in situ method) leads to slightly a better modulus, but it is in fact the presence or otherwise of agglomerates which is most important in failure properties (such as ductility). Poor dispersion results in organoclay agglomerates, which act as stress concentrators, leading to crack initiation when the tensile specimen is pulled apart. This is an important issue. Even though TEM may show broadly similar degrees of individual clay layer dispersion (which likely strongly effects modulus), the retention or otherwise of larger clay agglomerates (not seen in the very high magnifications of TEM, but rather by SEM) may be crucial to ultimate (failure) properties.

Acknowledgements

The authors would like to thank Dr Predrag Micic for providing the capillary rheology data. We also would like to acknowledge financial support from the Cooperative Research Centre for Polymers (CRC-P).

References

[1] Lan T, Pinnavaia TJ. Chem Mater 1994;6(12):2216–9.
[2] Prasad R, Pasanovic ZV, Gupta RK, Cser F, Bhattacharya SN. Polym Eng Sci 2004;44(7):1220–30.
[3] Hasegawa N, Kawasumi M, Kato M, Usuki A, Okada A. J Appl Polym Sci 1998;67(1):87–92.
[4] Kyu T, Zhu GC, Zhu ZL, Tajuddin Y, Qutubuddin S. J Polym Sci, Part B: Polym Phys 1996;34(10):1769–75.
[5] Tyan H, Liu Y, Wei KH. Polymer 1999;40(17):4877–86.
[6] Yano K, Usuki A, Okada A, Kurauchi T, Kamigaito O. J Polym Sci, Part A: Polym Chem 1993;31(10):2493–8.
[7] Kawasumi M, Hasegawa N, Kato M, Usuki A, Okada A. Macromolecules 1997;30(20):6333–8.
[8] Liu L, Qi Z, Zhu X. J Appl Polym Sci 1999;71(7):1133–8.
[9] Messersmith PB, Giannelis EP. Chem Mater 1994;6(10):1719–25.
[10] Vaia RA, Sauer BB, Tse OK, Giannelis EP. J Polym Sci, Part B: Polym Phys 1997;35(1):59–67.
[11] Alexandre M, Dubois P. Mater Sci Eng, R 2000;28(1–2):1–63.
[12] Cho JW, Paul DR. Polymer 2001;42(3):1083–94.
[13] LeBaron PC, Wang Z, Pinnavaia TJ. Appl Clay Sci 1999;15(1–2):11–29.
[14] Incarnato L, Scarfato P, Scatteia L, Acierno D. Polymer 2004;45:3487–96.
[15] Krishnamoorti R, Yurekli K. Colloid Interface Sci 2001;6:464–70.
[16] Pasanovic-Zujo V, Gupta RK, Bhattacharya SN. Rheol Acta 2004;43:99–108.
[17] Prasad R, Gupta RK, Cser F, Bhattacharya SN. J Polym Eng 2005;25(4):305–330.
[18] Krishnamoorti R. Polymer nanocomposites. New York, NY: Wiley; 2000 p. 315–343.
[19] Meissner J, Hostettler J. Rheol Acta 1994;33:1–21.
[20] Varlot K, Reynaud E, Kloppfer MH, Vigier G, Varlet J. J Polym Sci, Part B: Polym Phys 2001;39(12):1360–70.
[21] Devaux E, Bourbigot S, El Achari A. J Appl Polym Sci 2002;86(10):2416–23.
[22] Fornes TD, Paul DR. Polymer 2003;44:3945–61.
[23] VanderHart D, Asano A, Gilman JW. Chem Mater 2001;13(10):3781–95.
[24] VanderHart D, Asano A, Gilman JW. Chem Mater 2001;13(10):3796–809.
[25] Lincoln DM, Vaia RA, Wang ZG, Hsiao BS, Krishnamoorti R. Polymer 2001;42(25):9975–85.
[26] Hay JN, Shaw SJ. www.nano.org.uk/nanocomposites_review.pdf.